

Cross-sections for De-activation of $\text{Fe}(a^5D)$

BY A. B. CALLEAR AND R. J. OLDMAN

Physical Chemistry Laboratory, Lensfield Road, Cambridge

Received 16th May, 1967

Atomic iron was produced in a number of excited states by the isothermal flash-photolysis of $\text{Fe}(\text{CO})_5$. Relaxation rates between the spin-orbit multiplets of the a^5D states were measured in various gases by kinetic spectroscopy and plate photometry. The populations in the $J = 0, 1, 2$ and 3 states rapidly acquire a Boltzmann distribution, and subsequently undergo a comparatively slow relaxation to the ground a^5D state. The overall relaxation appears to be dominated by the rule $\Delta J = \pm 1$. The rate coefficients for the $J = 3 \rightarrow 4$ transition were recorded for relaxation by Ar, He, H_2 , D_2 , N_2 and CO; except for relaxation by Ar which is abnormally slow, the coefficients are of similar magnitude to those for deactivation of $\text{Se}(4^3P_0)$. Excited atomic iron and possibly $\text{Fe}^+(a^6D)$ reacted with O_2 and CO_2 to produce FeO , which was detected by the band at 2410 \AA .

We are presently investigating the collision-induced spin-orbit relaxation of some ground state atoms, and report here cross-sections for transitions between the $\text{Fe}(a^5D)$

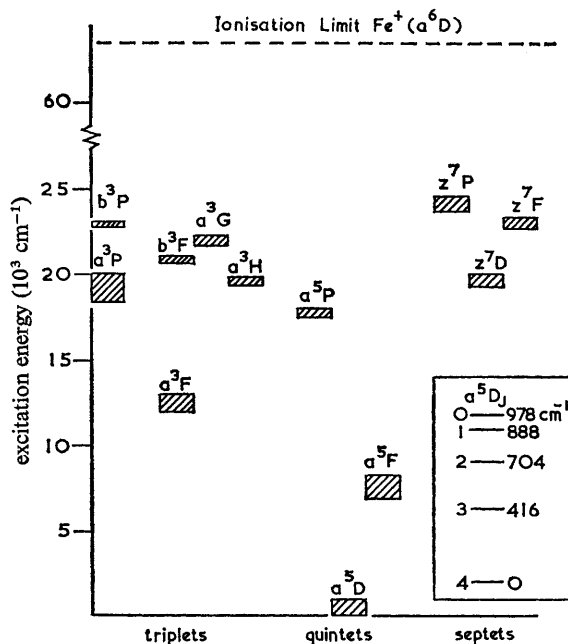


FIG. 1.—States of atomic iron detected in absorption in flashed $\text{Fe}(\text{CO})_5 + \text{Ar}$ mixtures.

multiplets. Two factors prompted a study of this atomic system. From the change of internal energy of the $J = 3 \rightarrow 4$ transition (416 cm^{-1}) and by analogy with the $\text{Se}(4^3P)$ system,¹ relaxation times were predicted to be in the range of access of kinetic

spectroscopy, at pressures where isothermal conditions can be maintained. Secondly, iron penta-carbonyl absorbs intensely in the ultra-violet, and when present at small partial pressures it can be entirely destroyed by the flash to provide, except for a trace of CO, a clean source of free atomic iron. The production of atoms requires multiple quantum absorption to remove successively the attached molecules of CO.² The subsequent state of the iron varies with time according to the four regimes: (i) during the flash, atoms excited to about 0.4 of the ionization potential were observed in absorption, together with iron ions. These highly excited species (fig. 1) decay with the exciting flash, and at 50 μ sec delay only the a^5D states are significantly populated. (ii) From 50–150 μ sec, the $J = 0, 1, 2$ and 3 a^5D substates acquire a Boltzmann distribution due to collisional coupling. (iii) From 150–800 μ sec, the coupled $J = 0-3$ system relaxes to the $J = 4$ ground state. (iv) At 1.5 msec, the atoms begin to polymerize at a rate which increases with increase in total pressure.

Our main objects have been to investigate the factors which control the establishment of equilibrium amongst the Fe(a^5D) states in an excess of Ar, and to measure the rate coefficients for the $J = 3 \rightarrow 4$ transition in various gases. The detection of highly excited atoms and ions is discussed in outline.

EXPERIMENTAL

Fe(CO)₅ (Mond Nickel Co.) was dried with anhydrous CuSO₄, degassed, and stored at 77°K. Cylinder Ar (British Oxygen Co.) was dried over P₂O₅ and kept in continual contact with reduced copper at 500°K. The absence of any significant concentration of N₂ in the Ar was demonstrated by observing the emission of N₂ bands from an electric discharge, and comparison with standard mixtures of N₂ and Ar. The other materials were all of research-grade purity, and were stored at 77°K. Mixtures of Fe(CO)₅ and Ar were prepared in glass bulbs protected from light. Practically all the experiments were conducted with 0.0010 mm of Fe(CO)₅ and 10–100 mm of inert gas. The vast excess of diluent limited the temperature change due to flashing to at most 5°K; occasional cleaning prevented the accumulation of precipitated iron which slightly reduces the transmission of the quartz after about 200 consecutive experiments.

TABLE 1.—ATOMIC LINES AND TRANSITION PROBABILITIES

transition X^5F	a^5D	wavelength (Å)	gA (10 ⁸ sec ⁻¹)		Beer-Lambert factor	
			ref. (3)	this work	30 mm Ar	100 mm Ar
5	4	2483.3	34	(34)	.59	.64
4	3	2488.1	35	35	.68	.57
3	2	2490.6	26	14	.67	.60
2	1	2491.2	15	6.5	.63	.61
1	0	2489.8	17	4.5	—	.58

The flash photolysis apparatus was of standard design. Absorption spectra were recorded with a medium quartz spectrograph, on Ilford HP3 plates which were developed for 2 min in Contrast FF diluted 1 : 4. The plate density change in the range 0.4–0.9 in the 2490 Å region, was accurately linear with log intensity (I). With a flash energy of 1670 J and an initial Fe(CO)₅ pressure of 0.001 mm, from the far u.-v. continuum the concentration was observed to fall to one half of the initial value after 5 μ sec, and the destruction of the reactant was effectively complete at 20 μ sec delay. Relative Fe(a^5D_J) concentrations were measured with the $a^5D_J \rightarrow x^5F_{J+1}$ transitions which are strong and comparatively free from interference due to other lines. The Beer-Lambert factor n in the expression

$$\log(I_0/I) = k(cl)^n$$

was determined for each of the five lines by blanking off $\frac{3}{4}$, $\frac{1}{2}$ and $\frac{1}{4}$ sections of the flash lamp and reaction vessel. The results are listed in table 1, together with relative transition probabilities which have been determined from the relative absorption of the five lines under

equilibrium conditions; the experimentally observed plate density changes were raised to the power of the reciprocal of the mean of the Beer-Lambert factors. Given also in table 1 are a set of published experimental transition probabilities,³ and our measurements have been normalized to the $J = 4$ line. At least part of the difference between the two sets of data is due to lack of complete resolution of the 2490.6 and 2491.2 Å lines, and because the resolution of the medium quartz spectrograph falls far short of that required to reproduce the true line contour. However, our data are in fair agreement with theoretical prediction.¹⁷

Within the errors of measurement, there is no significant variation of n from line to line, or with pressure. $n = 0.62$ has been employed in the analysis, and the uncertainty of ± 0.04 is included in the assessment of errors; all experiments were conducted at 293°K.

RESULTS

In fig. 2*a* are shown some of the transitions due to highly excited states of iron (table 2) which were detected in absorption; the concentrations of all levels above a^5D fall rapidly as the intensity of the flash decays. The formation and rapid decay

TABLE 2.—STATES OF ATOMIC IRON OBSERVED IN ABSORPTION

state	energy (cm ⁻¹)	state	energy (cm ⁻¹)
a^5D	0	a^3H	19,360
a^5F	6,928	b^3F	20,641
a^3F	11,976	a^3G	21,715
a^5P	17,550	Z^7F	22,650
a^3P	18,378	b^3P	22,838
Z^7D	19,350	Z^7P	23,711

of $\text{Fe}^+(a^6D)$ is illustrated in fig. 2*b*; the distribution of the ions in the spin-orbit multiplets changes with time and is initially non-Boltzmann. The total rate of decay of the ions increases with increase of the pressure of Ar. Iron ions can be produced by photo-ionization of some of the highly excited states of iron listed in table 2, since except for $\text{Fe}(a^5F)$ their ionization continua lie above 1850 Å. The concentration of atomic iron produced by the flash photolysis of $\text{Fe}(\text{CO})_5$ is independent of the flash energy provided the carbonyl is entirely destroyed. It was found experimentally that the ratios $[a^5D_3]:[a^5D_4]$ and $[a^5F]:[a^5D]$ are independent of flash energy for initial carbonyl pressures of 0.001 mm, which indicates that these states are populated directly by photolysis of carbonyl intermediates. However, the concentration of ions at short delay times was proportional to the flash energy, which is consistent with ionization of atomic iron by secondary light absorption. However, no detailed study of the kinetic behaviour of states other than $\text{Fe}(a^5D)$ has been attempted.

In fig. 3 the second and third phases of relaxation have been recorded. After 1 msec, the relative concentrations in the a^5D substates remain constant, and the relative absorption from the $J = 3$ and 4 lines divided by the transition probabilities, yielded a pressure-independent equilibrium temperature of $300 \pm 10^\circ\text{K}$. The time dependence of the photometered peak heights is given in fig. 4, and the ratios in fig. 5. The states $J = 0 \rightarrow 3$ have acquired a Boltzmann distribution by 150 μsec delay, and thereafter relax as a coupled system to the $J = 4$ ground state, until full equilibrium is established. In fig. 6 is plotted the dependence of the rate of the final $J = 3 \rightarrow 4$ step, on the pressure of Ar. There is a finite relaxation rate at limiting zero pressure of Ar. Each point of fig. 6 was derived from an assumed first-order decay, in the form of plots given in fig. 7 which also includes data for catalysis of energy transfer by added N_2 , CO, He, D_2 and H_2 .

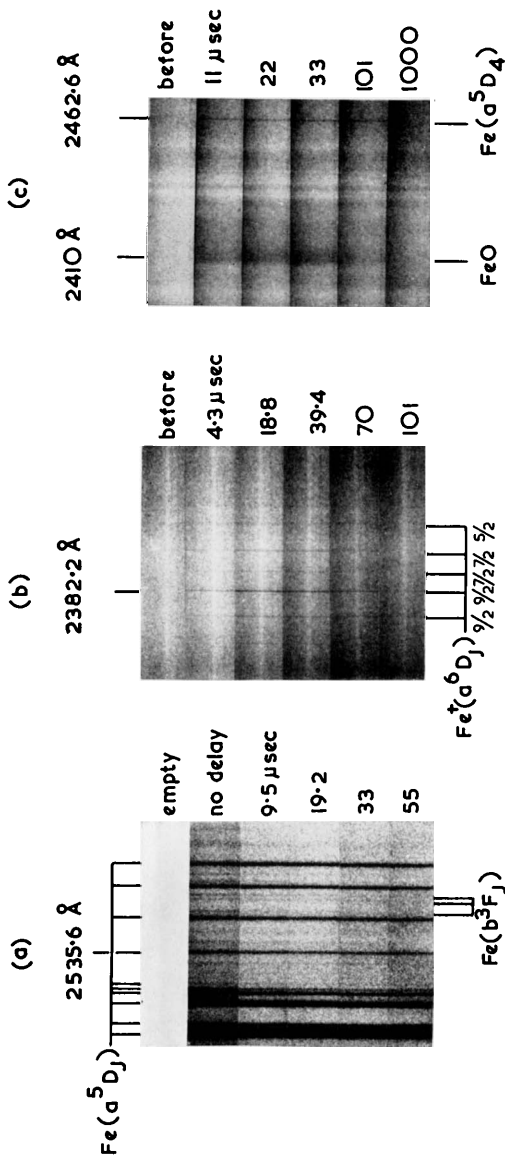


FIG. 2.—Transient spectra in flashed $\text{Fe}(\text{CO})_5$ vapour. (1670 J flash energy): (a) Formation and decay of $\text{Fe}(b^3F)$. 0.1 mm $\text{Fe}(\text{CO})_5 + 30$ mm Ar. (b) Relaxation and decay of $\text{Fe}^+(a^6D)$. 2×10^{-3} mm $\text{Fe}(\text{CO})_5 + 0.1$ mm $\text{O}_2 + 10$ mm Ar. (c) The 2410 Å FeO band. 2×10^{-3} mm $\text{Fe}(\text{CO})_5 + 0.1$ mm $\text{O}_2 + 10$ mm Ar.

[To face page 2890.

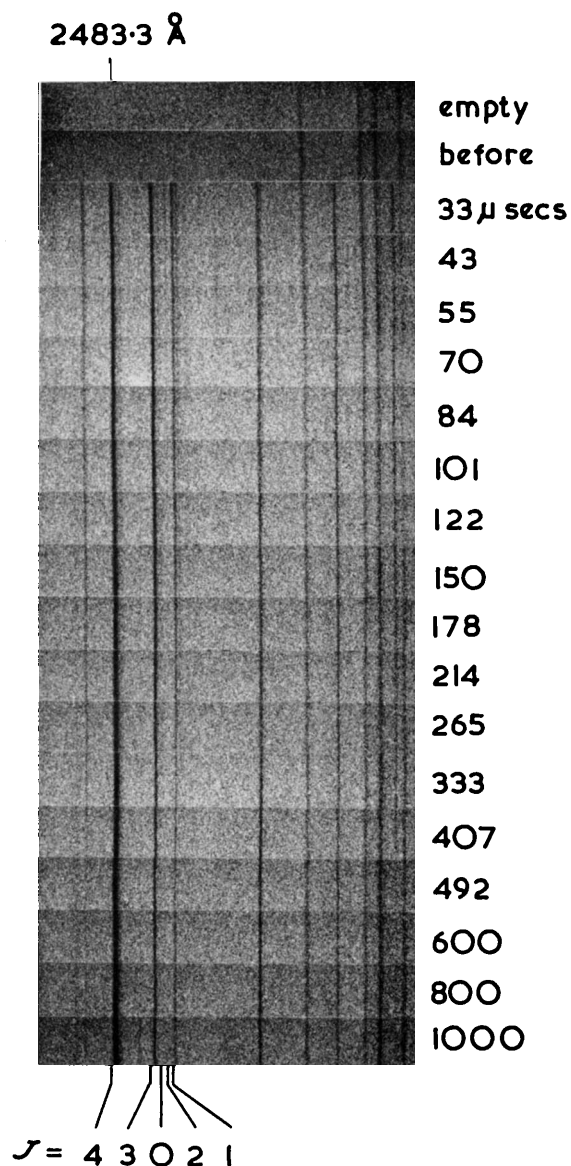


FIG. 3.—Production and relaxation of $\text{Fe}(a^5D_J)$. 50 mm Ar, 0.001 mm $\text{Fe}(\text{CO})_5$, 1670 J flash energy.

In the presence of CO_2 and O_2 , the band at 2410 \AA (fig. 2c) was observed; the same feature (though broadened to long wavelength) was detected in absorption in explosions containing iron additives by Callear and Norrish.⁴ The band is apparently

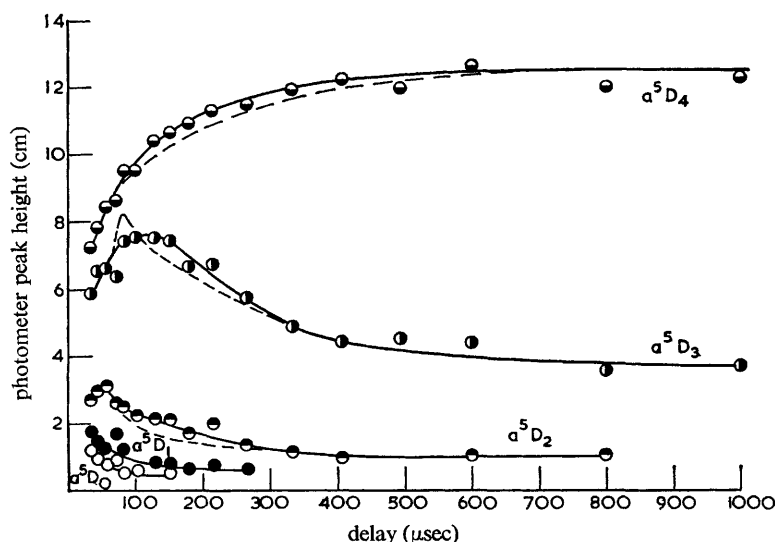


FIG. 4.—Spin-orbit relaxation of the $\text{Fe}(a^5D)$ multiplet. $0.001 \text{ mm Fe(CO)}_5 + 50 \text{ mm Ar}$. 1670 J flash energy. The broken lines were calculated from a one parameter model.

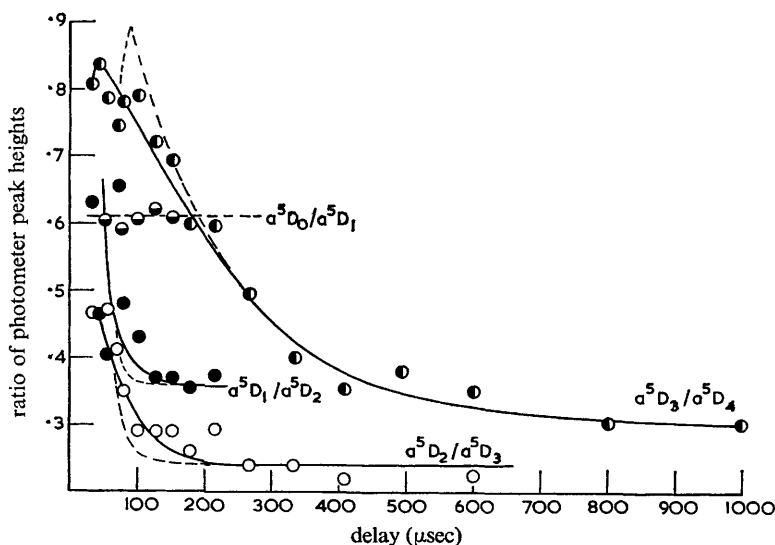


FIG. 5.—Variation of peak-height ratios with time. $0.001 \text{ mm Fe(CO)}_5 + 50 \text{ mm Ar}$. 1670 J flash energy. The broken lines were calculated from a one parameter model.

due to the FeO molecule, and the transition may be of the Rydberg type, occurring without change of nuclear separation. The intensity of the entire system reached a maximum with an O_2 or CO_2 pressure of $\sim 1 \text{ mm}$ and the decay rate increased rapidly with further increase of pressure. The rate of decay of the 2410 \AA band is not

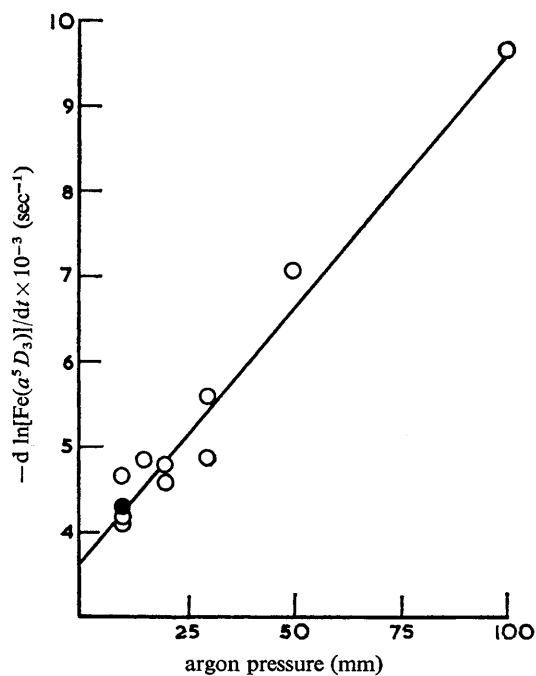
DE-ACTIVATION OF $\text{Fe}(a^5D)$ 

FIG. 6.—Relaxation of $\text{Fe}(a^5D)$ in argon. \circ , 1670 J flash energy; \bullet , 835 J.

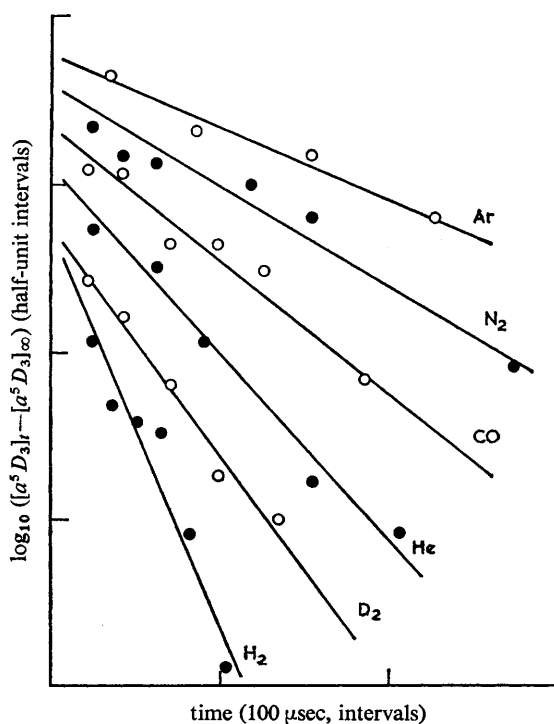


FIG. 7.—Semi-logarithmic plots (displaced for clarity) showing the decay of $\text{Fe}(a^5D_3)$ in 30 mm Ar with added gases. N_2 , 1 mm; CO , 0.05 mm; He , 5 mm; D_2 , 0.1 mm; H_2 , 0.1 mm.

significantly enhanced by increasing the Ar pressure. From consideration of the rates of relaxation and the extremely small concentration of FeO, the most reasonable interpretation is that the transition involves a low-lying state of the FeO molecule, but not the ground state. The rapid decay is due to relaxation by added O₂ and CO₂ and not due to chemical reaction. FeO may be produced by reaction of highly

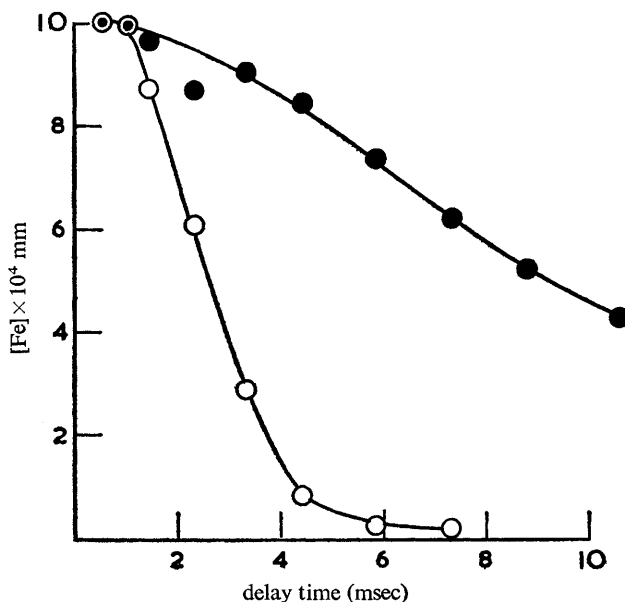


FIG. 8.—Decay of atomic iron by polymerization at two different pressures of argon. ●, 10 mm; ○, 100 mm.

excited atoms or iron ions with the oxygen containing additives. In the presence of the additives, the highly excited species and ions decay rapidly.

Fig. 8 shows the final decay of the total concentration of atomic iron, which is probably dependent initially on the three-body formation of Fe₂. CO₂, O₂ and N₂O greatly accelerate the rate of polymerization of atoms, and therefore accurate relaxation measurements could not be made in the presence of these gases.

DISCUSSION

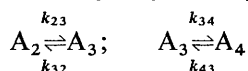
Some insight into the nature of the transitions may be obtained by consideration of the arguments of Zener,⁵ and of Jackson and Mott.⁶ For vibration-translation relaxation, the probability P of a transition is given by $16 \mu^2 V^2 T^2 / k_0 k_1 \hbar^4$. V is the vibrational matrix element, T is the translational overlap or tunnelling rate between the initial and final potentials, μ is the reduced mass of the system, and k_0 and k_1 relate to the relative speeds at large separation. Schwartz and Herzfeld⁷ have derived a similar result from a three-dimensional model. The empirical correlation of Lambert and Salter⁸ for vibrational relaxation essentially has its origin in the decreasing tunnelling probability with increasing separation between the initial and final potentials. Provided the potential may be expressed approximately as $V = f(x)g(\eta)$, where η is a function only of the electronic co-ordinates, and x is the nuclear separation (atom-atom collision), the same form for the transition probability may be retained, except that the resulting equation contains the square of the electronic matrix element. The separation of the electronic and nuclear co-ordinates

is reasonable for the processes presented because they have low probability, and only a small range of x , near the classical turning points, contributes to T . The main object of the discussion is to emphasize that the translational factor should be the same as that for $V-T$ and $V-V$ relaxation. The numerical value of this factor is extremely sensitive to the steepness of the intermolecular repulsion, and also the acceleration due to long-range attraction. However, we have deliberately attempted to choose molecular systems, spin-orbit relaxation of the lowest electronic states of atoms, for which the potential curves should be parallel (displaced by the internal energy change), for which the potential minima should not be appreciably in excess of kT , and for which the steepness of the repulsive potentials is comparable to that between stable molecules. We would then expect some correlation between these particular electronic processes, and other types of molecular energy transfer. The potential curves of the system will be parallel only where there is essentially little change of electronic structure, e.g., spin-orbit relaxation within a multiplet.

RELAXATION OF THE a^5D STATE

Fig. 4 and 5 show the two stages in the relaxation of the a^5D states; first, a rapid establishment of equilibrium in the upper four levels followed by the comparatively slow relaxation to the ground state. This behaviour is apparently a result of the disposition of the energy levels according to the Landé rule, such that the spacing between levels increases with J (fig. 1 inset). Since all five potential curves are approximately parallel, the rate coefficients decrease with increasing J . This also appears (a full derivation of all rate coefficients has not been achieved) to result in comparatively high cross-sections for $\Delta J = \pm 1$ transitions because they correspond to the smallest changes in internal energy. The "two stages" in the overall relaxation of a^5D have their origin in the same physical situation; the $J = 3 \rightarrow 4$ transition corresponds with the largest energy change and the rate coefficient k_{34} is small compared to those involving the higher J states. The notion of a "two stage" relaxation results partly from the lack of definition concerning the behaviour of the higher J states, because of limitations in the available range of gas pressures and the time resolution. The analysis by Phelps⁹ of the deactivation of the metastable states of neon shows several features in common with the $\text{Fe}(a^5D)$ system. There is also an analogue with the vibrational relaxation of poly-atomic molecules, which is generally controlled by the lowest vibrational frequency, because the energy difference between the lowest and next highest is usually a small fraction of the total vibrational quantum.

Before setting-up equations to describe the five level system, it is necessary to consider relaxation of a three level system which can be used to analyze the second stage to determine k_{34} . We first consider levels, 4 3 and 2, with energies of 0, E_3 and E_2 , with the condition that $E_2 - E_3 \ll E_3$. The processes may be abbreviated to



where the pseudo first-order coefficients k_{ij} represent the sum of the products of the second-order rate coefficients and the concentrations of relaxing gases. The general solution of the rate equations has the form

$$[\text{conc.}]_{J=i} = C_{i0} + C_{i1} \exp(\lambda_1 t) + C_{i2} \exp(\lambda_2 t),$$

where λ_1 and λ_2 are the roots of the determinant:

$$\begin{vmatrix} \lambda + k_{43} & -k_{34} & 0 \\ -k_{43} & \lambda + k_{34} + k_{32} & -k_{23} \\ 0 & -k_{32} & \lambda + k_{23} \end{vmatrix} = 0.$$

The solution is a two-stage relaxation; a fast equilibration of the levels 2 and 3 is followed by a comparatively slow final stage of coupling with the ground state. In this case, the values of -2λ are

$$\Sigma k_{ij} \pm ((\Sigma k_{ij})^2 - 4(k_{43}k_{32} + k_{43}k_{23} + k_{34}k_{23}))^{\frac{1}{2}}. \quad (1)$$

To a good approximation, the last stage of the relaxation of $\text{Fe}(a^5D)$ can be treated as the final stage of a three-level system, if the upper of the three levels is weighted (g) with the partition function of the $J = 0, 1$, and 2 states of $\text{Fe}(a^5D)$. Even in the three level system, the relaxation time of the final stage is only slightly dependent on k_{23} and k_{32} , and in a five-level system consisting of an inverted Landé multiplet, the final stage will show no significant dependence on the large rate coefficients which govern transitions between the three upper levels. This is evident experimentally by inspection of the data of fig. 4 and 5.

From the approximate correlation of cross-sections with internal energy change given later in fig. 9, the ratio $k_{23} : k_{34}$ is expected to be 20. (The experimental data

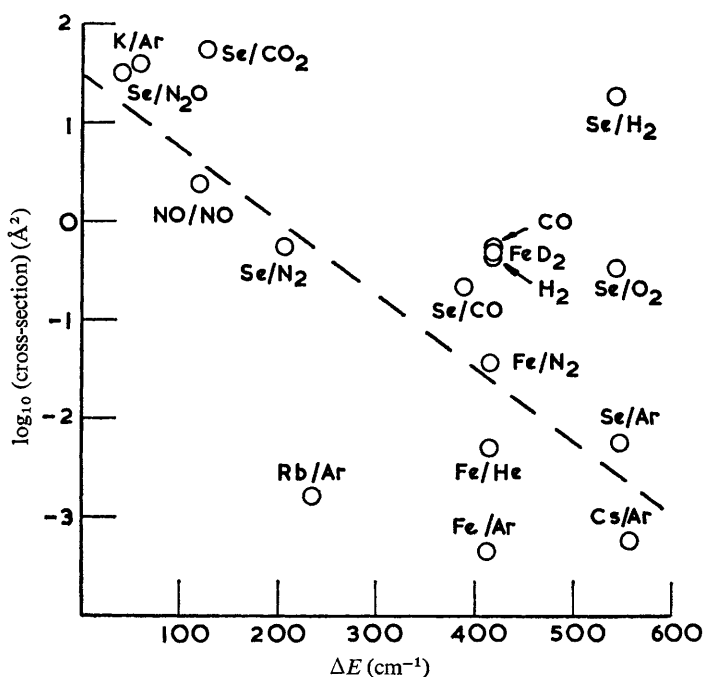


FIG. 9.—Diagram for spin-orbit relaxation.

indicate that this ratio is rather smaller (~ 10); however, the required λ value is not significantly changed.) By the principle of detailed balancing,

$$gk_{23} = 5k_{32} \exp [-(E_2 - E_3)/kT] \quad \text{and} \quad 9k_{34} = 7k_{43} \exp [-E_3/kT],$$

and substituting in (i) together with $k_{23} : k_{34} = 20$, it may be verified that the relaxation time τ of the final phase is related to k_{34} by the equation, $\tau = (0.91k_{34})^{-1}$. If the second stage is approximated to a two-level system (3 and 4 only), $\tau = (1.107k_{34})^{-1}$.

The second-order coefficients for the $3 \rightarrow 4$ transition can now be derived from the data of fig. 6. The form of the dependence of relaxation time on Ar pressure shows

that in addition to deactivation by Ar, there is at least one other major process involved. Addition of CO in quantities comparable to those released during photolysis, has no effect on the rates of relaxation. This seems to imply that the residual effect at limiting zero pressure of Ar is due to $\text{Fe} + \text{Fe}$ collisions, and would correspond to a deactivation cross-section of 23 \AA^2 . In this type of process, many potential curves intercept during collision to facilitate the occurrence of inelastic transitions. It was demonstrated that the intercept is approximately proportional to the initial concentration of carbonyl. Similar behaviour has been observed in self-collision of alkali metal atoms.¹⁰⁻¹² From the slope of fig. 6, $k_{\text{Ar}} = 2.1 (\pm 0.3) \times 10^{-15} \text{ cm}^3 \text{ sec}^{-1} \text{ molecule}^{-1}$ for the 3-4 transition.

Having established the total rate coefficient for the 3-4 transition, it is now possible to demonstrate that the observed behaviour of the five-level system is consistent with a theoretical model in which the rate coefficients depend inversely on the exponentials of the internal energy changes, and in which the selection rule $\Delta J = \pm 1$ is dominant. The general solution has the form

$$[\text{conc.}]_J = C_{10} + C_{11} \exp(\lambda_1 t) + C_{12} \exp(\lambda_2 t) + C_{13} \exp(\lambda_3 t) + C_{14} \exp(\lambda_4 t),$$

where the λ are the roots of the determinant :

$$\begin{vmatrix} \lambda + k_{43} & -k_{34} & 0 & 0 & 0 \\ -k_{43} & \lambda + k_{34} + k_{32} & -k_{23} & 0 & 0 \\ 0 & -k_{32} & \lambda + k_{23} + k_{21} & -k_{12} & 0 \\ 0 & 0 & -k_{21} & \lambda + k_{12} + k_{10} & -k_{01} \\ 0 & 0 & 0 & -k_{10} & \lambda + k_{01} \end{vmatrix} = 0$$

Rate coefficients have been approximated from k_{34} , by assuming the form,

$$\log k_{ij} = -A\Delta E_{ij} + B.$$

B was chosen to correspond to a rate coefficient at $\Delta E = 0$, equivalent to the gas kinetic cross-section. A was determined from the measured k_{34} . The roots of the above determinant were then derived numerically, together with the 15 coefficients C_{ij} . The computation was then initiated at $70 \mu\text{sec}$ with the observed concentrations, when the flash has terminated and when there is no significant population in states with greater energy than $\text{Fe}(a^5D)$. The dotted lines of fig. 4 are those calculated from the theory, and the fit with the experimental points indicates that the model is essentially correct. However, it is difficult to estimate $k_{24} : k_{23}$ from the data, and it is doubtful if the accuracy of the results merits a more elaborate analysis. Semiquantitative evidence for dominance of the $\Delta J = \pm 1$ transitions arises from a direct examination of the rates at which the adjacent substates achieve equilibrium.

RELAXATION BY ADDED GASES

The catalysis of the rate of the 3→4 transition by added gases is shown by the results of fig. 7. Relaxation times were measured in mixtures containing each of the added gases at four different concentrations, and the rate coefficients of table 3 have been derived from slopes of plots of $\log \tau^{-1}$ against gas concentration, and division by 0.91. The cross-sections are defined by the equation :

$$\text{cross-sections} = [\text{rate coef.}][\pi\mu/8kt]^{\frac{1}{2}}.$$

In fig. 9 the log cross-sections are plotted against change in internal energy, for $\text{Se}(4^3P)$, $\text{Fe}(a^5D)$ and $\text{NOX}^2\Pi^{13}$. The data of Krause and coworkers^{10, 14, 15} on spin-orbit relaxation of alkali metals by Ar, are also included. At least in collision with the inert gases, all these atomic transitions should occur between parallel

potentials, and with negligible attractive interaction. The broken line has the Lambert-Salter⁸ slope and has an intercept at $\Delta E = 0$ corresponding to the gas kinetic cross-section. The empirical line provides a rough indication of the limited tunnelling rate between parallel potential curves. Relaxation by Ar is abnormally slow with respect to this line, which apparently results from a weak coupling of the internal energy with translation. The interaction of the orbital angular momentum

TABLE 3.—RATE COEFFICIENTS AND CROSS-SECTIONS FOR THE DEACTIVATION $\text{Fe}(a^5D_{3 \rightarrow 4})$; 293°K

gas	rate coef. ($\text{cm}^3 \text{ sec}^{-1} \text{ molecule}^{-1}$)	cross-section (cm^2)
Ar	$2.1 \pm .3 \times 10^{-15}$	4.1×10^{-20}
N ₂	$1.9 \pm .3 \times 10^{-13}$	3.5×10^{-18}
He	$6.2 \pm .7 \times 10^{-14}$	4.7×10^{-19}
CO	$2.9 \pm .5 \times 10^{-12}$	5.0×10^{-17}
H ₂	$7.4 \pm .7 \times 10^{-12}$	4.1×10^{-17}
D ₂	$6.1 \pm .7 \times 10^{-12}$	4.7×10^{-17}
Fe	$1.1 \pm .2 \times 10^{-10}$	2.3×10^{-15}

with the axial field of the nuclei does not efficiently re-orient the spin-orbit coupling.¹⁶ The cross-section for relaxation of $\text{Rb}(5^2P_J)$ ¹⁵ is also abnormally small. The He cross-sections are generally greater than those of Ar, and part of this difference seems to be due to the reduced mass effect which is well established in vibrational energy transfer. It is due to the greater translation overlap or tunnelling rate of the light molecule which has a comparatively long wavelength for a given energy.

Diatomic molecules are considerably more efficient than inert gas atoms at inducing spin-orbit relaxation. The $\text{Fe} + \text{N}_2$ and $\text{Se} + \text{N}_2$ results correlate well with the Lambert-Salter line, and the CO results are slightly high. The greater efficiency of the diatomic molecules is probably due to a more complex electronic coupling to the field of all three nuclei. The causes of differences in the behaviour of Fe and Se are obscure; e.g., why does H_2 relax $\text{Se}(4^3P_0)$ about a 100 times faster than it relaxes $\text{Fe}(a^5D_3)$?

We are indebted to the Science Research Council for the award of a studentship to R. J. Oldman. We acknowledge stimulating discussions with Dr. R. J. Cvetanović.

¹ A. B. Callear and W. J. R. Tyerman, *Trans. Faraday Soc.*, 1966, **62**, 2313.

² A. B. Callear and R. J. Oldman, *Nature*, 1966, **210**, 730.

³ C. H. Corliss and B. Warner, *Nat. Bur. Stand. J. Res. A*, 1966, **70**, 325.

⁴ A. B. Callear and R. G. W. Norrish, *Proc. Roy. Soc. A*, 1961, **259**, 304.

⁵ C. Zener, *Physic. Rev.*, 1931, **37**, 556.

⁶ J. M. Jackson and N. F. Mott, *Proc. Roy. Soc. A*, 1932, **137**, 703.

⁷ R. H. Schwarz and K. F. Herzfeld, *J. Chem. Physics*, 1954, **22**, 767. K. F. Herzfeld and T. A. Litovitz, *Absorption and Dispersion of Ultrasonic Waves* (Academic Press, New York, 1959).

⁸ J. D. Lambert and R. Salter, *Proc. Roy. Soc. A*, 1957, **253**, 280.

⁹ A. V. Phelps, *Physic. Rev.*, 1959, **114**, 1011.

¹⁰ G. D. Chapman and L. Krause, *Can. J. Physics*, 1966, **44**, 753.

¹¹ M. Czajkowski and L. Krause, *Can. J. Physics*, 1965, **43**, 1259.

¹² A. G. A. Rae and L. Krause, *Can. J. Physics*, 1965, **43**, 1574.

¹³ H. J. Bauer, H. O. Kneser and E. Sittig, *J. Chem. Physics*, 1949, **30**, 1119.

¹⁴ M. Czajkowski, D. A. McGillis and L. Krause, *Can. J. Physics*, 1966, **44**, 731.

¹⁵ B. Pitre, A. G. A. Rae and L. Krause, *Can. J. Physics*, 1966, **44**, 731.

¹⁶ J. W. Moskowitz and W. R. Thorson, *J. Chem. Physics*, 1963, **38**, 1848.

¹⁷ E. U. Condon and G. H. Shortley, *The Theory of Atomic Spectra* (Cambridge University Press, 1953), p. 242.